Air optical breakdown on silicon as a novel method to fabricate photoluminescent Si-based nanostructures

A. V. Kabashin*, M. Meunier
Ecole Polytechnique de Montréal, Département de Génie Physique, Case Postale 6079, succ. Centre-ville, Montréal (Québec), Canada, H3C 3A7

ABSTRACT

A novel "dry", vacuum-free laser-assisted method for a fabrication of nanostructured Si/SiO_x layers on a silicon wafer is demonstrated. This method uses the phenomenon of air optical breakdown to modify a semiconductor surface. Pulsed radiation from a CO_2 laser was focused on a silicon wafer to initiate the optical breakdown in atmospheric pressure air. After several breakdown initiations near the threshold of plasma production, a gray-tint layer was formed under the radiation spot on the silicon surface. The size of the processed area could be controlled by varying the radiation focusing conditions. Properties of the layers were studied by optical and SEM microscopies, XPS, XRD, Specular X-ra Reflectivity and PL spectroscopy. It was found that the layers had the porosity of about 75-80% and contained nanoscale holes and channels. They consisted of silicon nanocrystals embedded in S $_2$ matrix and exhibited strong photoluminescence (PL) at 1.9-2.0 eV, which could be seen by naked eyes. Possible mechanisms of nanostructur formation and PL origin are discussed. The method can be used for a controlled local patterning of photoluminescent nanostructured materials.

Keywords: air optical breakdown, nanostructured silicon, visible photoluminescence, CO_2 laser processing.

1. INTRODUCTION

An implementation of optoelectronics technology on silicon basis is of great importance for the development of a new generation of low-cost photonic devices and their integration in standard Si-based microelectronics platform. However, bulk silicon has an indirect and small band gap (1.11 eV at room temperature) and does not emit visible light, which limits dramatically its application in the area of optoelectronics devices. The search of methods for the production of visible light-emission from Si-based materials becomes currently a great task and a subject of numerous studies (see, e.g., Refs. 1-14).

It has been recently shown that silicon and Si-based compounds become luminescent in the visible range when the undergo size reduction to the nanometer dimensions. This nanostructuring could be produced b anodical etching of a silicon wafer in HF solutions [1] or by a deposition of nanocluster Si-based films through different "dry" methods such as, for example, magnetron sputtering [2], laser breakdown of silane[3], pulsed laser ablation[4-8] etc. Though the anodical etching enables one to produce nanostructured silicon with the most intense photoluminescence emission, "dry" fabrication methods are considered as more adequate for creating optoelectronics devices due to their better potential compatibilit with silicon processing technology.

Dry deposition techniques generally imply a formation of a thin nanostructured film on a substrate. However, in some cases it is important to produce local nanostructured area directly on a silicon-based device or an assembled integrated chip. One of the possibilities is a local annealing by pulsed radiation from an excimer laser of an amorphous Si-based film below the plasma initiation threshold[9,10]. Using this method, nanostructured areas exhibiting PL in red (1.65 eV) and green (2.2 eV) were patterned, but the method required a preliminary deposition of the amorphous film, which made it

* akabach@email.phys.polymtl.ca; phone 1-(514)340-4711 ext. 4634, Ecole Polytechnique de Montréal, Département de Génie Physique et Groupe de recherche en physique et technologie des couches minces (GCM), Case Postale 6079, succ. Centre-ville, Montréal (Québec), Canada, H3C 3A7

rather expensive. Another possible approach is the processing of a silicon wafer by an electric spark[11-14]. Here, a silicon wafer is used as a cathode in a plasma-assisted process, in which unipolar discharges between two electrodes ionize the gaseous environment and accelerate the generated ions toward the silicon surface transforming it to a nanostructured Si-based layer. The processed material was found to exhibit strong photoluminescence in UV/blue (3.22 eV) and green (2.36 eV) spectral ranges and relatively weak and unstable PL in the red (1.9 eV) range[14]. The method is "dry" and not expensive since it does not require any vacuum system. However, this technique is relatively slow and usually requires several hours of processing to achieve efficient PL emission. In addition, it uses high voltages, which can damag electronic circuit of a processed chip.

In this paper, we demonstrate another dry and vacuum-free method for the local patterning of nanostructured Si-based materials on a silicon wafer. This method uses the phenomenon of air optical breakdown to modify a silicon target and thus produce a layer of photoluminescent material on its surface. In the presented study, the main attention is given to the visible and near-infrared ranges of the spectrum (S-band), which are known to be the most important fo optoelectronics applications.

2. EXPERIMENTAL ARRANGEMENT

In the experiments, radiation of a pulsed TEA CO_2 laser (wavelength 10.6 µm, pulse energy 1 J, pulse length 1 µs FWHM, repetition rate 3 Hz) was focused by a Fresnel's lens (focal length of 5 cm) near a silicon target as shown in Fig. 1. The radiation intensity was about 10^8 W/cm^2 at the focal plane. Standard silicon wafers (N- and P-type, resistance 0.01- 10 Ohm·cm) with dimensions about 1×1 cm^2 were used as targets. They were placed in different positions from z = -20 mm to z = 20 mm, where z = 0 corresponds to the focal plane. Experiments were carried out in atmospheric air (1 atm, 20° C, 40% humidity).

The PL spectra were measured at room temperature using a double spectrometer (model U100, Instruments SA) and a GaAs photomultiplier Hamamatsu Photonics). The samples were illuminated by the radiation of a cw Ar^+ laser (model INNOVA 100) with the wavelength 488 nm. The power was 10 mW and the power density was estimated to be 30 W/cm^2. The spectra were corrected to take into account the spectral response of the PL setup. Scanning Electron Microscopy (SEM) was used to examine structural properties of the films. The surface composition of the layers was analyzed by X-ray photoemission spectroscopy (XPS) using a Thermo VG Scientific System. In addition, X-ra diffraction (XRD) and Specular X-ray Reflectivity[15] (SXRR) spectroscopies were used to examine the crystallinity and the porosity of the films.

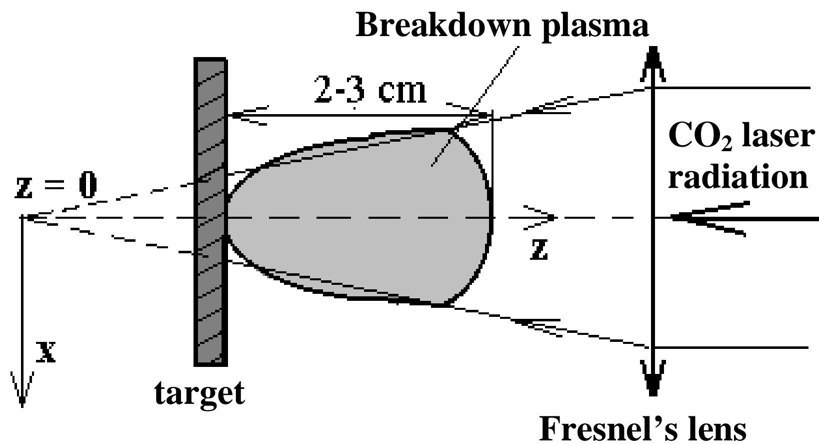

Fig. 1 Schematic of experimental setup.

3. RESULTS

3.1 Conditions of air optical breakdown processing

First of all, it was found that the breakdown initiation threshold depends on the efficiency of radiation absorption by the upper target surface layer. In particular, relatively high radiation power was required to ignite the breakdown on a clean silicon wafer. However, the threshold was significantly lower when the radiation spot stroke on a dust or contaminant on the silicon surface. After the breakdown ignition, the plasma intensity raised progressively with the number of laser shots on the same spot and stabilized only after 20-100 shots, corresponding to 10-30 seconds of treatment. The intensity gain was apparently connected to the production of mechanical defects on the target surface, which improved the radiation absorption. In our experiments, the treatment was performed under near-threshold conditions to minimize possible deposition of material on the surrounding free target surface.

After breakdown initiations by several laser pulses, a gray-tint area was formed under the focal spot on the silicon surface. The size of this area depended on radiation spot size, which was mainly determined by the target position with respect to the focal plane of the focusing lens. Changing this position from $z = -20$ mm to $z = 0$ mm, the size of the area could be varied from hundreds of microns to millimeters

3.2 SEM study

As shown on the SEM image of Fig. 2, the silicon surface treated by 10 laser shots contained nanoscale holes, between 30 and 150 nm in diameter. However, smaller pores, not resolved by SEM, may still be additionally present. A prolonged treatment of the silicon surface led to a formation of columns and channels with similar dimensions. For samples treated under the threshold of plasma initiation, SEM studies did not detect the presence of the ablated material outside the treated area on the free target surface.

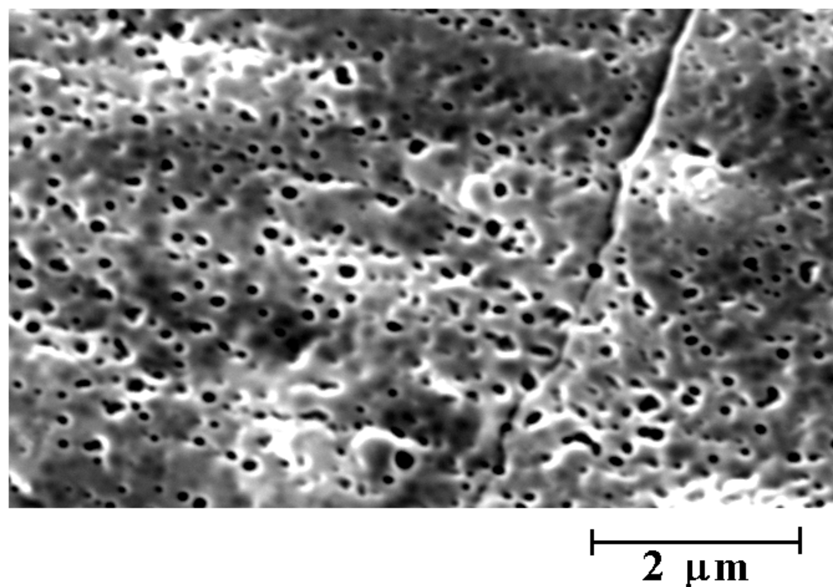

Fig. 2. Typical SEM image of a silicon target surface under the radiation spot after 10 breakdown initiations near the plasma ignition threshold.

3.3 XPS study

To understand better the essence of air optical breakdown treatment, the surface composition of the layers was examined by X-ray photoelectron spectroscopy (XPS). The spectra of all samples demonstrated a single peak at about 104 eV, as shown in Fig. 3. This peak is always assigned to 2p photoelectrons of pure SiO_2, suggesting that the processed laye mainly consisted of silicon dioxide. It should be noted that the layers obtained by electric spark processing of silicon also consisted of silicon dioxide[11,13]. This gives evidence for similar mechanisms of surface treatment in these two cases.

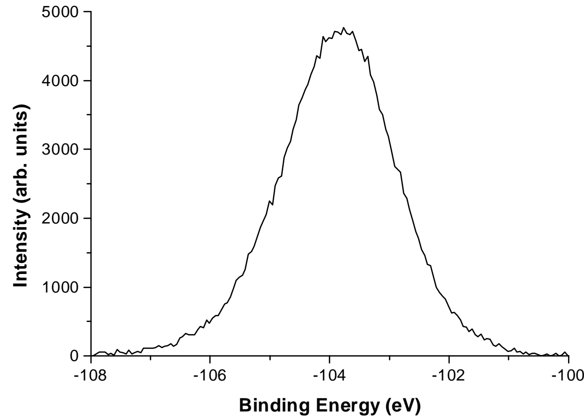

Fig. 3. Typical XPS spectrum from the Si/SiO_x layers produced by air optical breakdown processing.

3.4 XRD study

X-ray Diffraction spectra were recorded to determine whether silicon crystals are present in the treated layer. Fig. 4 (a) shows typical spectra from a silicon target before and after the optical breakdown processing. One can see that th treatment led to the appearance of additional XRD peaks associated with different crystalline silicon lines. This gives the evidence that the resulting layers consisted of silicon crystals embedded in SiO_2 matrix. It is know [16] that th broadness of XRD peaks is mainly determined by the smallest clusters. As the instrumental noises are relatively low, this property could be used to estimate the minimal size of crystals in the deposit by the Debye-Scherrer formula[16]. Taking the broadness of a typical silicon peak ($\Delta(2\theta)/2 = 0.6$ deg.) from a highly resolved XRD spectrum (Fig. 4 (b)), the estimation gives the grain size of the order of 10 nm.

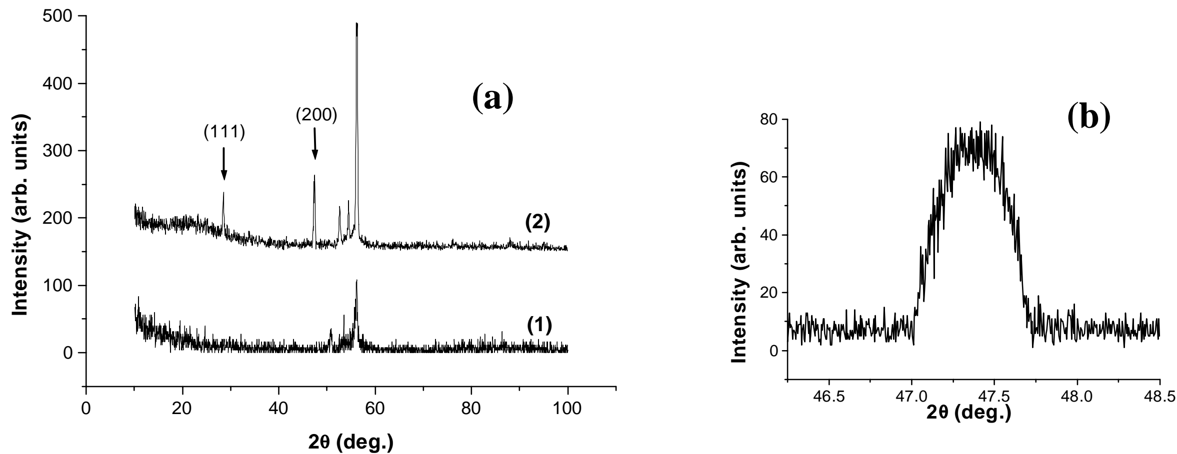

Fig. 4. (a) Typical XRD spectra before (spectrum 1) and after (2) the breakdown processing of a silicon wafer [N-type, (1,0,0), 10 Ohm·cm]. To enhance XRD signal, a rectangular area with dimensions of 5×5 mm^2 was treated on a silicon wafer by shifting the laser beam over the target.
(b) Highly resolved XRD spectrum near a crystalline silicon line

3.5 SXRR study

It was concluded from SEM studies that the layers represented highly porous material with significant fraction of holes and channels. To characterize quantitatively the porosity of the layers, we used a technique of Specular X-ra Reflectivity (SXR)[15]. SXRR spectra were obtained with the use of an X-ra diffractometer, which made possible a monitoring of the intensity of X-ray beam reflected from a surface under a simultaneous θ-2θ scanning of a source and a

detector (0°<θ<1°, θ was measured towards the surface). Since for X-rays the refractive index of most materials is less than 1, a phenomenon of total external reflection occurs for $\theta < \theta_c$, while fo $\theta > \theta_c$ the reflected intensity suffers a rapid attenuation. Taking into account that θ_c is proportional to the square root of the electronic density, which is directl proportional to the density of the material, the porosity can be determined from the critical angle measurements by the following formula:

$$porosity(\%) = 100\left(1 - \frac{\theta_c^2}{\theta_{c\,bulk\,Si}^2}\right) \tag{1}$$

where θ_c and $\theta_{c\,bulk\,Si}$ are the critical angles from SXRR spectra for a thin film and bulk silicon, respectively.

Experimental reflectivity curves for a silicon target before and after the treatment are presented in Fig. 5. One can see that the critical angle $\theta_{c\,bulk\,Si}$ for the substrate before the treatment (curve 1) was about 0.22°. Similar substrate-related critical angle of 0.22° could be observed after the treatment. However, the treatment led to the appearance of an additional air/layer interface-related critical angle θ_c of about 0.1-0.11° as shown in Fig. 5 (curve 2). Substituting the values of $\theta_{c\,bulk\,Si}$ an θ_c into equation (1), we obtain the film porosities of 75-80%.

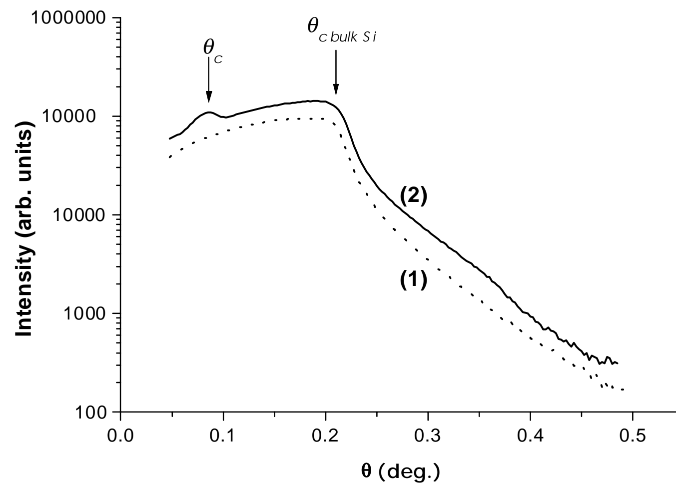

Fig. 5 Typical SXRR spectra before (spectrum 1) and after (2) the breakdown processing. The later spectrum was collected from the treated area with the dimensions 5×5 mm^2. Each point of the area was treated by at least 100 laser pulses.

3.6 PL study

The processed area exhibited strong PL signals, which could be easily seen by naked eyes. Fig. 6 shows that a typical PL spectrum from the breakdown-treated area had a main emission band in red range around 1.9-2.0 eV. The peak position was independent of the extent of the surface treatment, type of silicon wafer (N- or P-) and doping level, corresponding to resistances varying from 0.01 to 10 Ohm·cm. Our experiments showed that the PL signals were relatively stable to a prolonged illumination of the layers by the radiation of an Ar^+ laser. In particular, the decrease of their integral intensit did not exceed 40% even after 6 hours of the continuous illumination.

4. DISCUSSION

It is known that the optical breakdown produced by infrared radiation can be divided approximatel into three successive phases[17]. During the first phase, the target generates initial electrons and the ionization develops in a cold gas. The

second phase is characterized by the interaction of the 1 μs laser pulse with the breakdown plasma, whose shock wave propagates in air from the target toward the focusing lens.

The main radiation is absorbed at the forefront of the shock wave through the inverse Bremsstrahlung mechanism. A some moment, the plasma becomes hardly transparent to oncoming radiation and gets heated up to the temperatures of about 10^4 K, while the laser-related ablation of material almost stops. After the laser pulse, the shock wave transforms to a gradually decaying "fireball", which can live several milliseconds and is characterized by an intense light emission, generation of ultra-strong currents (with magnitudes up to 10^6 A)[18] and appearance of various electromagneti phenomena[19-21].

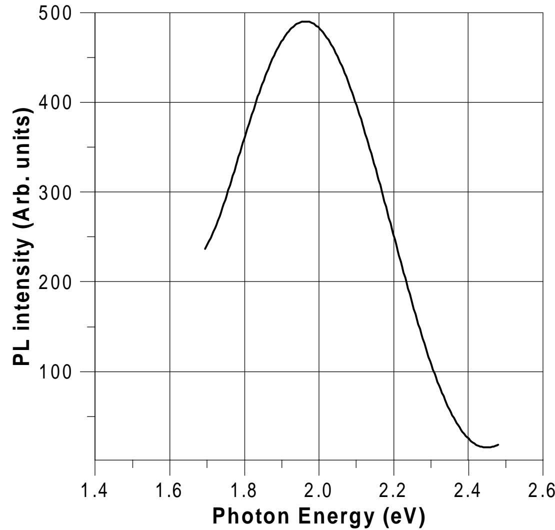

Fig. 6. Typical photoluminescence spectrum from the central part of Si-based layer fabricated by the breakdown processing of a silicon wafer [P-type, (1,0,0), 0.01 Ohm·cm) by hundreds of laser shots at the same focal spot.

In our opinion, the action of radiation during the first and second phases can lead to a localized melting and even flash evaporation of the target material, which causes properties modification. Since the radiation is pulsed, one can assume recrystallization or local vapo redeposition of the material during the off-times. Another possible mechanism of the material modification may be related to the breakdown plasma itself. This plasma, heated to high temperature (10^4 K) and presenting intense currents (10^6 A), can additionally heat the laser-evaporated particles or even the upper target layer, thus modifying the properties of formed silicon-related compounds. It is necessary to note that our SEM studies did not reveal any remarkable redeposition of material on the surrounding free target surface, which is typical for conventional pulsed laser ablation with UV radiation[4-8]. Such a difference of deposition efficiencies is probably connected with quit different mechanisms of radiation absorption in these two cases. In contrast to the infrared light case, the main UV radiation power is absorbed by the target itself and the plasma remains transparent to the oncoming light during the laser pulse. This causes a considerable laser-related ablation of material during the interaction and it redeposition on the free target surface.

It seems that the mechanism of surface treatment in our experiments is similar in many respects to that of the electric spark processing, which was also used for the fabrication of Si-based nanostructured layer [11-14]. The spark-treated silicon also contained 10-500 nm holes and pores and consisted of silicon nanocrystals embedded in SiO_2 matrix (the presence of nanometer-size crystals was confirmed by Transmission Electron Microscopy studies[13]). The modifications wer attributed to pulsed ion bombardment of silicon surfaces, which led to a flash evaporation of the target material and its recrystallization during the off-times. Furthermore, the nanostructured layers fabricated by the electric spark processing in pure oxygen also exhibited 1.9 eV signals[11,12,14], though they were relatively weak and fast-degrading[14]. However, the origin of these signals is still under debate. The generation of 1.9 eV PL band is frequently ascribed to radiative

transitions via non-bridging oxygen hole centers[22]. However, detailed analysis of similar 1.9 eV signals and their properties in the case of spark-processed silicon does not confirm this assumption [13,14]. Other possible mechanism is a radiative recombination between quantum confined states in the nanoscale particles[1], which was involved to explain some properties of the 1.9 eV component in the case of spark-processed silicon[12]. In any case, a clear identification of the PL mechanism requires further detailed study of mechanical, structural and PL properties of the deposited and annealed films. These investigations are in progress.

4. CONCLUSION

In summary, air optical breakdown has been produced on a silicon target for local nanostructuring of its material. We showed that the breakdown production led to the formation of porous layer under the radiation spot, which consisted of silicon nanocrystals imbedded in S $_2$ matrix and exhibited strong red PL. The method can be used for a controlled local patterning of photoluminescent nanostructured materials.

ACKNOWLEDGEMENTS

The authors are grateful to R. Leonelli for assistance during PL studies, and to S. Poulin for the XPS measurements.

REFERENCES

1. L. T. Canham, “Silicon quantum wire array fabrication by electrochemical and chemical dissolution of wafers”, *Appl. Phys. Lett.*, **57**, pp. 1046-1048, 1990.
2. H. Takagi, H. Ogawa, Y. Yamazaki, A. Ishizaki, and T. Nakagiri, “Quantum size effects on photoluminescence in ultrafine Si particles”, *Appl. Phys. Lett.*, **56**, pp. 2379-2380, 1990.
3. Y. Kanemitsu, T. Ogawa, K. Shiraishi, and K. Takeda, Visible photoluminescence from oxidized Si nanometer-sized spheres: exciton confinement on a spherical shell”, *Phys Rev. B*, **48**, pp. 4883-4886, 1993.
4. I. A. Movtchan, R. W. Dreyfus, W. Marine, M. Sentis, M. Autric, G. Le Lay and N. Merk, “Luminescence from a Si-SiO_x nanocluster-like structure prepared by laser ablation”, *Thin Solid Films*, **255**, pp. 286-289, 1995.
5. Y. Yamada, T. Orii, I. Umezu, Sh. Takeyama, and T. Yoshida, “Optical properties of silicon nanocrystallites prepared by excimer laser ablation in inert gas”, *Jpn. J. Appl. Phys., Part 1*, **35**, pp.1361-1365, 1996.
6. T. Makimura, Y. Kunii, and K. Murakami, “Light emission from nanometer-sized silicon particles fabricated by the laser ablation method”, ”, *Jpn. J. Appl. Phys., Part 1*, **35**, pp.4780-4784, 1996.
7. A.V. Kabashin, M. Charbonneau-Lefort, M. Meunier, and R. Leonelli, “Effects of deposition and post-fabrication conditions on PL properties of nanostructured Si/SiOx films prepared by laser ablation”, *Appl. Surf. Sci.*, **168**, pp. 328-331, 2000.
8. A.V. Kabashin, M. Meunier, and R Leonelli, “Photoluminescence characterization of Si-based nanostructured films produced by laser ablation”, *J. Vac. Sci. Tech. B*, **19**, pp. 2217-2222, 2001.
9. K. M. A. El-Kader, J. Oswald, J. Koka, and V. Chab, Formation of luminescent silicon by laser annealing of a-Si:H, *Appl. Phys. Lett.,* **64,** pp. 2555-2557, 1994.
10. K. M. A. El-Kader et. al., “The influence of preparation conditions on the PL spectra of light-emitting Si prepared by pulse irradiation of a-Si:H”, *Thin Solid Films*, **276**, pp. 306-309, 1996.
11. R.E Hummel, S-S. Chang**, “**Novel technique for preparing porous silicon”, *Appl. Phys. Lett.,* **61**, pp. 1965-1967, 1992.
12. E.F. Steigmeier, H. Auderset, B. Delley, and R Morf, “Visible light emission from Si materials*”, J. Luminescence,* **57,** pp. 9-12, 1993.
13. R.E. Hummel, A. Morrone, M. Ludwig, and S .-S. Chang, “On the origin of photoluminescence in spark-eroded (porous) silicon”, *Appl. Phys. Lett.*, **63,** pp. 2771-2773, 1993.
14. M.H. Ludwig, A. Augustin, and R.E. Hummel, “Colour-switching effect of photoluminescent silicon after spark-processing in oxygen”, *Semicond. Sci. Technol.*, **12,** pp. 981-986, 1997.
15. L. T. Parratt, “Surface studies of solids by total reflection of x-rays”, *Phys. Rev.,* **95**, pp. 359-369, 1954.
16. B. D. Cullity, *Elements of X-ray diffraction* (Addison-Westle , Reading, MA, 1978).

17. Yu.P. Raizer *Laser-Induced Discharge Phenomena* (Consultants Bureau, New York, 1977).
18. M.G. Drouet, and H. Pepin, "Parametric study of the current induced in a CO_2 laser plasma", *Appl. Phys. Lett.*, **28,** pp. 426-431, 1976.
19. V.V. Korobkin, and R.V. Serov, "Spontaneous magnetic fields of laser spark", *Pis'ma Zh. Eksp. Teor. Fiz.* **4,** pp. 103-107, 1966 [*JETP Lett.* **4**, pp. 70-75, 1966].
20. A.V. Kabashin, and P.I. Nikitin, "Electric fields of a laser spark produced by radiation with various parameters", *Quant. Electronics,* **27,** pp. 536-542, 1997.
21. A.V. Kabashin, P.I. Nikitin, W. Marine, and M. Sentis, "Experimental study of spontaneous electric field generated by a laser plasma", *Appl. Phys. Lett.* **73,** pp. 25-27, 1998.
22. S. Munekuni, T. Yamanaka, Y. Shimogaichi, K. Nagasawa, Y. Hama, " Various types of nonbridging oxygen hole center in high-purity silicon glass", *J. Appl. Phys.*, **68**, pp. 1212-1217, 1990.